摩擦学学报
TRIBOLOGY

粗糙氧化锆涂层对多晶锆表面摩擦性能的影响

向友文，张晓宇，王政慧，匡陶，蒲超，史义超

Impact of Rough Zirconia Coating on the Surface Friction Properties of Polycrystalline Zirconia

XIANG Youwen, ZHANG Xiaoyu, WANG Zhenghui, KUANG Tao, PU Chao, SHI Yichao

在线阅读 View online: https://doi.org/10.16078/j.tribology.2023216

向友文, 张晓宇, 王政慧, 匡陶, 蒲超, 史义超. 粗糙氧化锆涂层对多晶锆表面摩擦性能的影响[J]. 摩擦学学报(中英文), 2025, 45(3): 421−430. XIANG Youwen, ZHANG Xiaoyu, WANG Zhenghui, KUANG Tao, PU Chao, SHI Yichao. Impact of Rough Zirconia Coating on the Surface Friction Properties of Polycrystalline Zirconia[J]. Tribology, 2025, 45(3): 421−430. DOI: 10.16078/j.tribology.2023216

粗糙氧化锆涂层对多晶锆表面摩擦性能的影响

向友文[1], 张晓宇[1*], 王政慧[2], 匡 陶[1], 蒲 超[1], 史义超[1]
(1. 西南交通大学 机械工程学院, 四川 成都 610031;
2. 西南交通大学 数学学院, 四川 成都 610031)

摘 要: 采用分子动力学方法模拟了金刚石半球与具有不同粗糙度氧化锆表面涂层的多晶锆基体的磨削过程, 对摩擦力、摩擦系数、磨损量和磨损深度进行了定量分析并且结合应力应变、位错提取分析法(DXA)和热力学分析法对基体内部塑性变形进行了探究. 结果表明: 随着氧化锆涂层粗糙度的增加, 压头磨削方向与涂层和基体的实际接触面积减小导致其相互作用力减小, 涂层对其法向的反作用力增大, 导致压头所受的摩擦力逐渐减小, 基体磨损原子量减少及磨损深度降低. 经DXA分析, 基体内部压头下压区域都产生堆垛层错, 但亚表层损伤程度及内部晶格缺陷结构随着粗糙度的增加相应减弱.

关键词: 多晶锆; 分子动力学; 摩擦磨损; 涂层; 粗糙度
中图分类号: TH117.1 **文献标志码:** A **文章编号:** 1004-0595(2025)03–0421–10

Impact of Rough Zirconia Coating on the Surface Friction Properties of Polycrystalline Zirconia

XIANG Youwen[1], ZHANG Xiaoyu[1*], WANG Zhenghui[2], KUANG Tao[1], PU Chao[1], SHI Yichao[1]

(*1. School of Mechanical Engineering, Southwest Jiaotong University, Sichuan Chengdu 610031, China;*
2. School of Mathematics, Southwest Jiaotong University, Sichuan Chengdu 610031, China)

Abstract: Zirconium alloys are widely used in the nuclear industry due to their excellent mechanical properties. The grid and cladding tubes in fuel rods of nuclear voltage water reactors often experience micro motion wear between equipment due to oscillations generated by coolant flowing through the pipelines. Moreover, the material is prone to oxidation and the formation of an oxide film on its surface when exposed to complex environments, such as high temperature, high pressure and corrosion for a long time, greatly reducing its service life. Although the precision of material processing is getting higher and higher nowadays, the surface roughness of materials can be achieved to be very small. However, the influence of the roughness of the two contact surfaces on friction and wear can not be ignored at the microscopic level. Therefore, the W-M fractal theory was used to establish zirconia coatings with different roughness levels (D=2.3, 2.4, 2.5, 2.7, 2.8). Molecular dynamics simulations were used to simulate the grinding process of diamond hemispheres and polycrystalline zirconia substrates with different roughness levels. Quantitative analysis was conducted on friction force, friction coefficient, wear amount, and wear depth, and combined with stress-strain, dislocation extraction analysis (DXA), and thermodynamic analysis methods to explore the plastic deformation inside the matrix. The results showed

Received 10 October 2023, revised 21 January 2024, accepted 22 January 2024, available online 18 June 2024.
*Corresponding author. E-mail: zhangyu3035@126.com, Tel: +86-13880418157.
This project was supported by the National Natural Science Foundation of China (51775459) and Key R&D Projects in Sichuan Province (23ZDYF0375).
国家自然科学基金项目(51775459)和四川省重点研发项目(23ZDYF0375)资助.

that as the roughness of the zirconia coating increased, the friction force and average friction coefficient showed a decreasing trend. The actual contact area between the grinding direction of the indenter and the coating and substrate decreased, resulting in a decrease in their interaction force. The normal reaction force of the coating on it increased, leading to a gradual decrease in the friction force on the indenter; The atomic weight of the substrate decreased and the wear depth decreased, resulting in weakened adhesion and plowing effects during the wear process. Indicating that an increase in roughness could significantly improve the surface wear resistance of polycrystalline zirconium and reduce the damage to the sub surface of the matrix. According to DXA analysis, there were fewer areas of stress concentration on the surface of the matrix, and the depth of transmission was shallower. Stacking faults were generated in the areas under the pressure of the internal pressure head of the matrix. However, the degree of sub surface damage and the internal lattice defect structure weakened correspondingly with the increase of roughness. The total potential energy showed a trend of first increasing and then decreasing, $E_{C\text{-}C}$ showed an upward trend, and $E_{C\text{-}Zr}$ showed a downward trend. $\Delta E_{C\text{-}Zr}$ showed a downward trend, $\Delta E_{Zr\text{-}Zr}$ showed a downward trend, $\Delta E_{C\text{-}C}$ had no significant change pattern. Research had shown that when designing zirconia coatings with the same coating thickness, a zirconia coating with higher roughness could enhance the wear resistance of polycrystalline zirconia matrix and reduce the degree of damage to the matrix material during grinding.

Key words: polycrystalline zirconium; molecular dynamics; friction and wear; coating; roughness

锆(Zirconium, Zr)金属具有较小中子吸收截面、良好的高温力学性能及抗腐蚀性能，被应用于核电设备的关键零部件包壳管[1-2]. 在核电系统中，包壳管处于恶劣的服役环境中，由于快速流动高温高压水作用，导致定位格架的弹簧/刚凸与燃料棒包壳之间发生幅度极小的相对运动，从而使包壳管发生磨损现象，导致管壁局部损伤以及破裂，使用寿命降低，危及核电安全[3]. 因此，开展有关研究工作，探索损伤机理用以预测和防止核燃料包壳管过早破损，延长其使用寿命具有重要意义.

近年来国内外学者已经研究过大量的锆合金表面涂层技术工艺与材料，包括陶瓷材料、FeCrAl合金、Cr系合金和MAX相等[4-7]，FeCrAl合金本身具有抗高温氧化的特性，但在事故下存在界面失效的风险；MAX相是1类具有六方晶体结构的纳米层状化合物，其化学式可以表示为$M_{n+1}AX_n$，其中M代表前过渡金属元素，A代表主族元素(主要为13-15主族元素)，X代表碳或氮元素，n通常取值为1、2或3，MAX相涂层可以通过不同的方法使其具备抗高温氧化的特性，但其在长期的辐照环境下的运行稳定性还需考量；Van Nieuwenhove等[8]使用CrN、TiAlN和AlCrN这3种涂层包覆的燃料棒进行了堆内试验，结果表明CrN涂层在反应堆辐照环境下稳定性最优；Shah等[9]在应变条件下对涂层结构完整性及Cr涂层对锆基体的力学性能影响进行了研究，其结果发现Cr涂层未出现开裂现象，达到包壳管力学材料性能要求；Li等[10]研究了MAX相材料涂层，试验后发现材料表面生成3层致密氧化膜. 但实际工作环境中，锆合金表面本身会形成1层氧化锆保护膜，并且氧化锆(ZrO_2)涂层是1种具有优良的隔热性、耐磨性以及优异力学性能的陶瓷材料涂层[11]. 从摩擦学设计角度出发，探讨不同因素对摩擦磨损失效的有效控制，为减缓界面破坏提供理论支持.

目前针对锆合金表面涂层技术的研究主要集中于涂层的工艺选择、力学性能以及耐磨性和耐腐蚀性等方面[12-13]，大量学者从宏观角度出发，研究了涂层技术对锆合金摩擦行为的影响[14-15]，但受试验观测技术的限制，对上述磨损现象内在的作用机制缺乏深入理解.

随计算机技术快速发展，运用微观尺度分子动力学模拟(Molecular dynamics simulation，MDS)方法可从原子尺度对摩擦磨损过程进行深入解析[16]，研究宏观试验较难获取的磨损原子、基体塑性变形以及内部缺陷结构等问题，且分形理论的应用使得MDS能模拟真实的粗糙表面摩擦，试验结果更加符合实际[17]. 故本文中采用MDS方法，研究不同粗糙度ZrO_2表面涂层材料的摩擦学行为和微观磨损机制.

1 模型建立与参数设置

1.1 模型建立

使用Atmosk[18]软件集成的Voronio tessellation (泰森多边形算法)建立基体，基体为多晶锆，晶格参数为a=0.3234 nm，c=0.5168 nm，晶粒个数为30个，平均晶粒尺寸为5.46 nm. 将基体分为3个区域，分别为固定层、温控层和牛顿层. 在Matlab中使用Majumdar[19]等基于G-W模型创建的Weierstrass-Mandelbrot (W-M)[20]分形函数建立粗糙ZrO_2涂层. 涂层为ZrO_2晶粒模型，其对应的晶粒参数为a=0.3600 nm，b=0.3600 nm，c=

0.5225 nm. 使用分形维数D来表征涂层表面的粗糙度，分形维数反应了粗糙体对空间的占据程度以及粗糙体表面的复杂程度，其值越大粗糙体越复杂，宏观下基体的平均粗糙度R_a和均方根粗糙度R_q越大. 图1所示为不同粗糙度的ZrO_2涂层，压头为1个刚性金刚石半球体，模型总体三维尺寸如图2所示.

1.2　模拟参数设置

本文中分子动力学模拟采用开源软件Lammps (Large-scale atomic/molecular massively parallel simulator)[21]. 整个系统采用NVT系综并使用Langevin控温法对整个系统进行控温，时间步长为2 fs，使用Velocity-Verlet算法对原子运动方程求解. 此外，为了消除尺寸效应对模拟结果的影响，在X和Y方向采用周期性边界条件.

合适的势函数是保证模拟结果准确的前提，本文中采用在MDS中广泛使用的Tersoff势函数[22]来描述压头中C原子之间的相互作用，采用EAM势函数[23]来描述多晶锆基体中Zr原子之间的相互作用，采用Morse势函数[24]来描述压头中C原子与基体Zr原子之间的相互作用，其表达形式简单. 具体表达式如下：

$$V(r) = -D_e + D_e(1 - e^{-\alpha(r-r_e)})^2 \tag{1}$$

式中，r_e表示2个原子之间的平衡距离；r表示两原子间的距离；D_e表示势井深度；α表示势井宽度. 本文中其参数取值分别为D_e=1.56 eV，α=3.3786 Å^{-1}，r_e=2.1187 Å. 采用Buckingham势函数[25]描述ZrO_2涂层之间的作用力，A_{ij}代表原子间能量，ρ_{ij}代表原子间距离，C_{ij}代表原子间能量与距离的比值. 具体势参数列于表1中[26].

为消除初始模型构建时的误差对模拟结果准确性的影响，在模拟之前对整个系统进行200 000时间步长(200 ps)的弛豫. 模拟过程分为下压和磨削两部分，下压过程对压头施加544 nN的法向载荷，在弛豫一段时间后设置磨削速度为1.0 Å/ps，磨削距离为130 Å. 整个模拟过程的参数设置汇总列于表2中.

1.3　模拟分析方法

摩擦力分析在摩擦磨损模拟中起着关键作用，通

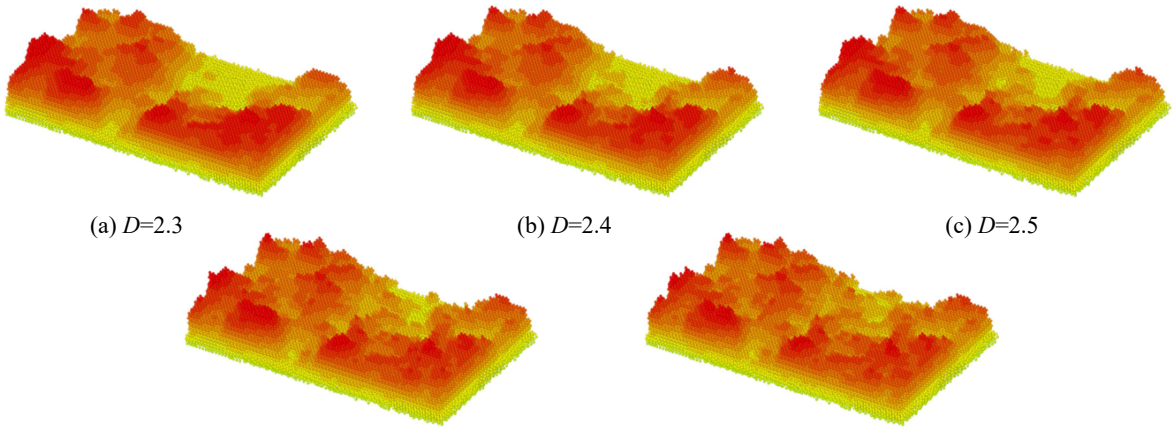

Fig. 1　ZrO_2 coatings with different roughness

图 1　不同粗糙度的ZrO_2涂层

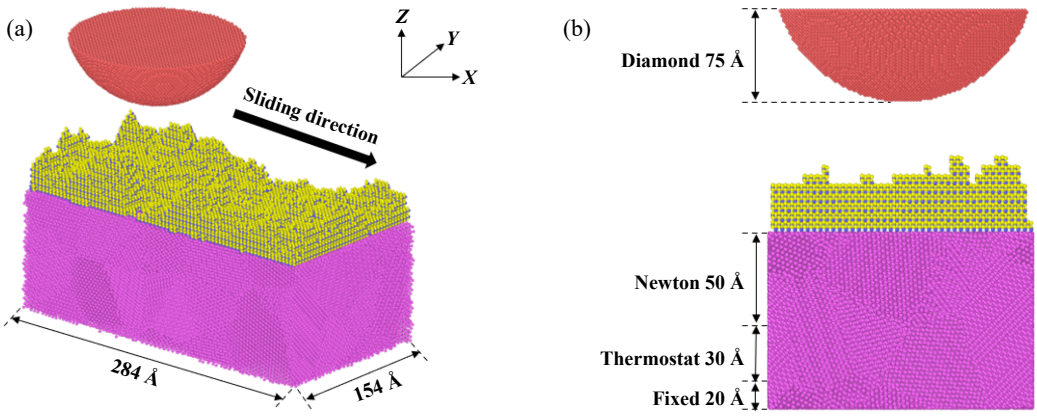

Fig. 2　Overall 3D view of the model: (a) overall dimensions of the model; (b) left view of the model

图 2　模型整体三维图: (a)模型整体尺寸; (b)模型左视图

表 1 ZrO2晶体的势参数[26]
Table 1 Potential parameters of ZrO_2 crystals

Atomic pair	A_{ij}/eV	ρ_{ij}/Å	C_{ij}/(eV/Å^5)
Zr-O	985.87	0.376	0.000
O-O	22764.30	0.149	2.789
Zr-Zr	0.00	0.000	0.000

表 2 模拟过程的参数设置
Table 2 Parameter settings for simulation process

Parameter	Specifications
Time step/fs	2
Ensemble	NVT
Temperature/K	300
Boundary condition (*XYZ*)	PPF
Sliding distence/Å	130
Load/nN	544
Sliding velocity/(Å/ps)	1
Potential	Tersoff (C-C), EAM (Zr-Zr), Morse (C-Zr), Buckingham (ZrO_2), Lennard-Jones

过摩擦力的定量分析并结合基体内部塑性变形，有助于对摩擦磨损机理的深入理解. 本文中摩擦力定义为压头在滑移方向上原子所受到力的总和. 相比于传统试验，磨损量在MDS中较容易获得，本文中通过原子的位移阈值[27]是否超过24 Å来判定其是否为磨损原子. 磨损深度定义为压头的质心到基体平面之间的法向垂直距离，数值越大磨损深度越小.

磨削过程中常伴随着基体塑性变形，塑性变形又是由位错的滑移产生. 本文中借助可视化软件OVITO中的位错提取分析方法(DXA, Dislocation extract analysis)[28]、共邻分析法(CNA, Common neighbor analysis)[29]和原子应变分析法(Atomic strain analysis)[30]对磨削过程中基体内部塑性变形进行分析.

2 试验结果与分析

2.1 摩擦力分析

图3所示为摩擦力及摩擦系数曲线图，从图3(a)中可以看出由于基体表面的不均匀性、材料间的黏附和剥离等原因，导致摩擦力曲线持续波动，最终动态稳定. 从摩擦力曲线可以看出整个磨削过程大致分为3个过程：(1) 0~2 nm磨削初始阶段，涂层与基体的大量变形导致摩擦力的急剧增大；(2) 2~10 nm磨削持续阶段，磨损原子在压头前方堆积导致摩擦力缓慢上升；(3) 10~13 nm磨削稳定阶段，此时磨损原子的堆积与分离达到了动态平衡，摩擦力也在一定范围内维持动态平衡.

从摩擦力曲线与摩擦系数曲线可以看出，摩擦力随着粗糙度的增加逐渐减小，摩擦系数随之降低，Si与Li在其粗糙模型的试验中也观察到相同的现象[31-32]. 随着粗糙度的增加，压头磨削方向与涂层和基体的实际接触面积(图4中压头空缺部分为接触面积)减小导致其相互作用力减小，如图4所示.

2.2 磨损量及磨损深度分析

分析磨损量和磨损深度可以评估材料性能和耐磨性，如图5所示，随着粗糙度的增加，磨损量逐渐减小，磨损深度降低，这与Zhu等[33]研究中的结论一致. 纳米尺寸下的摩擦力可划分为三部分：黏附力($F_{adhesion}$)、犁耕力($F_{plouging}$)和磨损原子阻力(F_{chip})，表达式如下：

$$F_{friction}=F_{adhesion}+F_{plouging}+F_{chip} \quad (2)$$

式中，犁耕力的大小与磨损原子量息息相关，磨损原子量又决定了磨损原子阻力的大小. 可见随着涂层粗糙度的增加，ZrO_2涂层对压头法向的反作用力增加，导致磨损深度减小，犁耕效应减弱，对应上式中的$F_{plouging}$和F_{chip}相应地减小. 图6所示为Z轴方向上90~

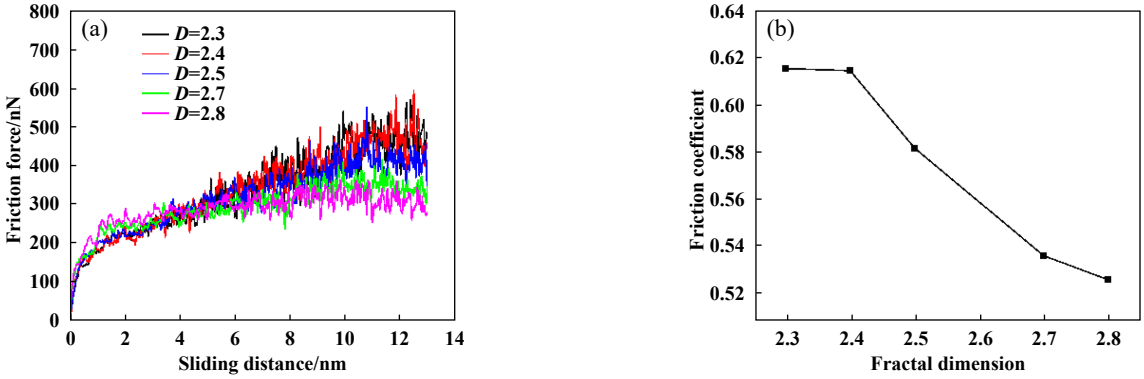

Fig. 3 Friction force and friction coefficient under different roughness ZrO_2 coatings: (a) friction force; (b) average friction coefficient

图 3 不同粗糙度ZrO_2涂层下的摩擦力与摩擦系数：(a)摩擦力；(b)平均摩擦系数

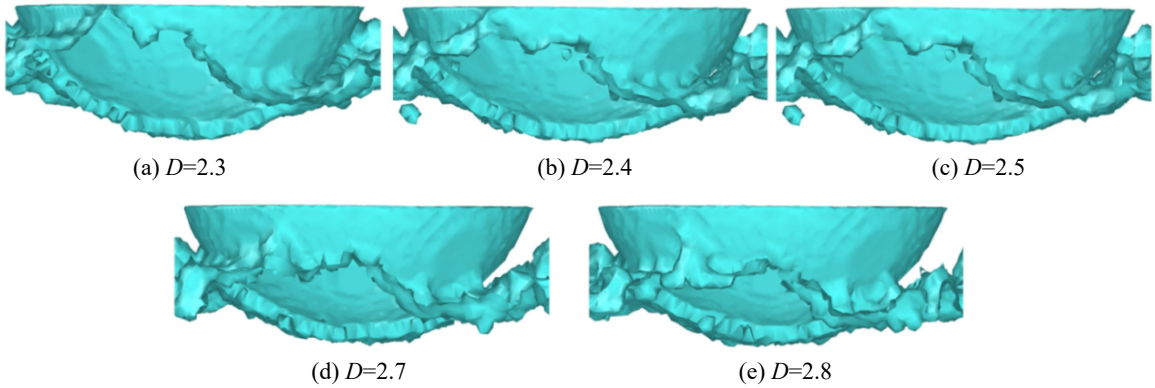

(a) D=2.3　(b) D=2.4　(c) D=2.5

(d) D=2.7　(e) D=2.8

Fig. 4　Contact area between the indenter and the substrate in the X-direction

图 4　压头与基体X方向接触面积

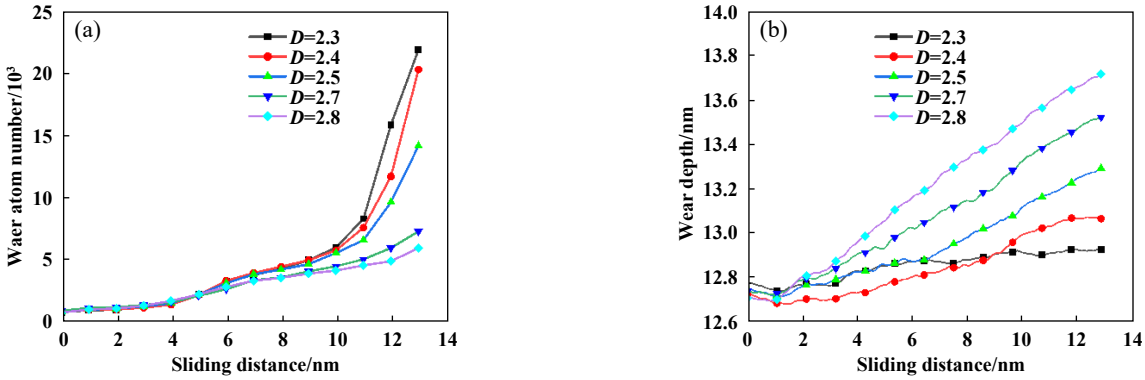

Fig. 5　Wear atom number and wear depth under different roughness ZrO_2 coatings: (a) wear atom number; (b) wear depth

图 5　不同粗糙度ZrO_2涂层下的磨损原子量与磨损深度: (a)磨损原子量; (b)磨损深度

140 Å的基体磨损原子分布图, 由图6可知, 随着ZrO_2涂层粗糙度的增加, 基体亚表层的磨损原子减少, 磨削轨迹上的磨损原子也相应减少, 压头与基体间的黏附效应减弱, 可见越粗糙的ZrO_2涂层越能增强基体的耐磨性.

2.3　基体内部变形机理分析

分析摩擦力、磨损量和磨损深度是从宏观的角度理解摩擦过程中材料的变化, 想要深入的理解材料的摩擦磨损机理还需对其内部塑性变形进行分析. 在磨削过程中, 压头正下方的区域发生的塑性变形最严重, 故截取Y方向+77 Å的截面进行分析. 本文中从应力应变、塑性变形和热力学3个方面对基体内部的塑性变形进行分析.

2.3.1　应力应变分析

图7所示为随着涂层粗糙度的增加, 相同的载荷下基体内部的应力分布有明显的差异, 0~1表示剪切应力逐渐增大. Area A为压头下压区域, 可以看出此区域发生了严重的塑性变形, 同时在磨削过程中, 亚表层晶界处还存在连续的剪切应力. 比较D=2.3和2.8的表面应力集中区域与压头前方区域(Area B)可以发现随着粗糙度的增加, 涂层对压头的反作用力增大, 降低了应力传导, 应力在基体中传递的深度更浅, 发生的塑性变形更少.

2.3.2　塑性变形分析

在磨削过程中, 位错的产生主要是应力集中、外力作用、晶界滑移和晶体缺陷等原因导致的. 如图8所示, 在基体的压头下压区域, 应力的高度集中导致不同粗糙度的ZrO_2涂层基体都出现了堆垛层错的形核和扩展, 且形核和扩展的方向大致相同. 但是在D=2.3和2.5的基体中, 磨削结束后压头前方基体中都产生了堆垛层错, 随着粗糙度的继续增大, 相同区域并未观察到堆垛层错的产生. 由此可见, 涂层粗糙度的增加, 应力传递更浅, 导致基体内部的堆垛层错和位错等缺陷结构减少, 亚表层的损伤程度减小, 这与前文中磨损原子减少, 基体损伤程度以及耐磨性的增加相对应.

2.3.3　内部能量分析

采用热力学方法对磨削过程中能量变化进行分析, 本文中采用NVT系综进行模拟, 故模拟过程中系统的总动能(E_k)保持恒定, 主要分析系统的势能变化(E_p). E_p

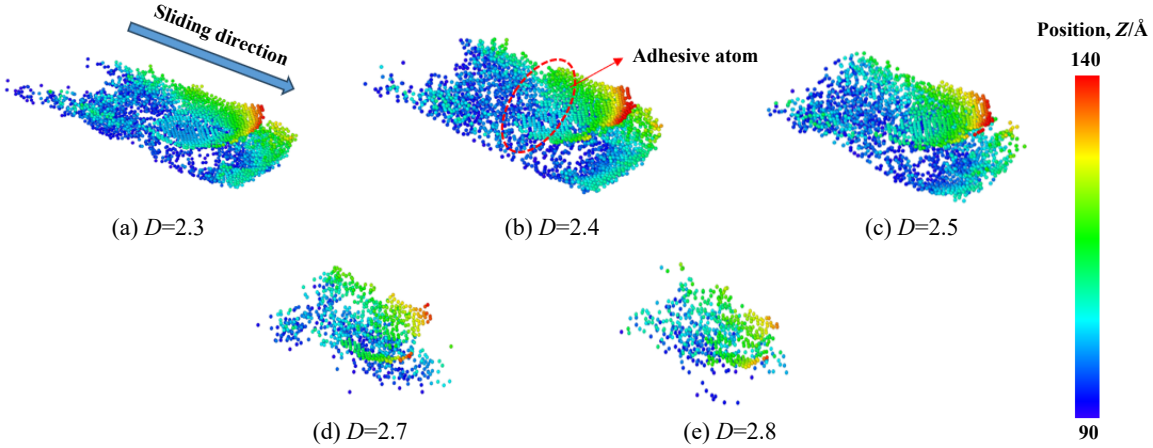

Fig. 6 Distribution of wear atoms in the substrate of ZrO_2 coatings with different roughness

图 6 不同粗糙度ZrO_2涂层下基体的磨损原子分布图

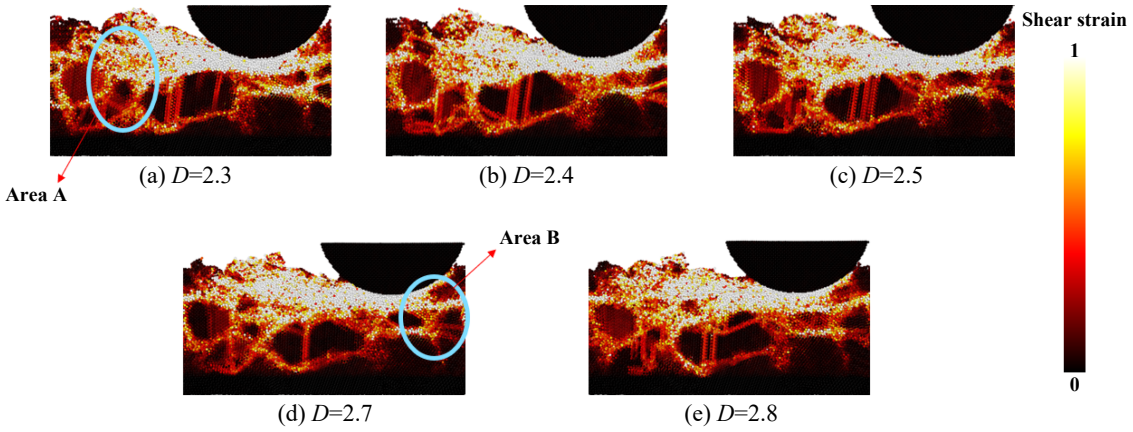

Fig. 7 Stress distribution of the substrate under different roughness ZrO_2 coatings

图 7 不同粗糙度ZrO_2涂层下基体的应力分布图

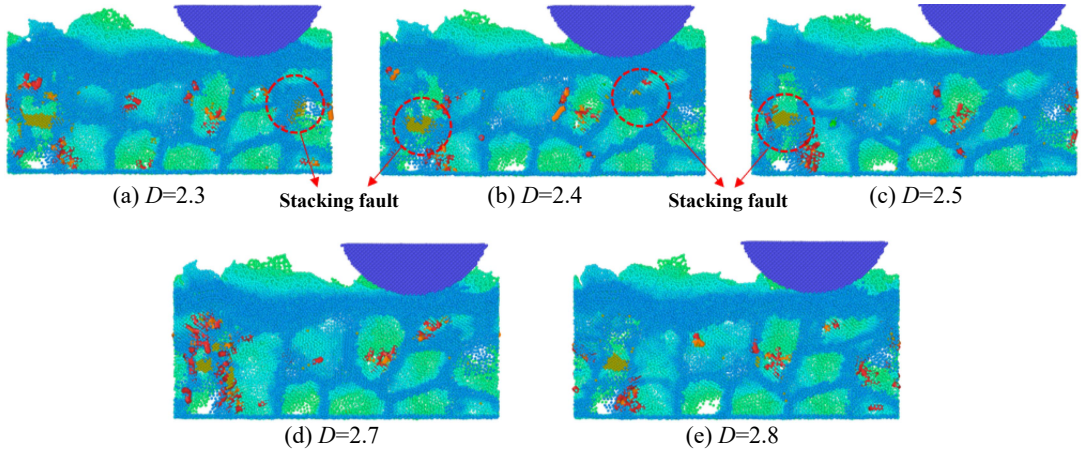

Fig. 8 DXA analysis of the substrate under different roughness ZrO_2 coatings

图 8 不同粗糙度ZrO_2涂层下基体的DXA分析图

主要由三部分组成:C原子间势能($E_{C\text{-}C}$)、C和Zr原子间势能($E_{C\text{-}Zr}$)以及Zr和Zr原子间势能($E_{Zr\text{-}Zr}$). 其表达式为

$$E_p = E_{C\text{-}C} + E_{C\text{-}Zr} + E_{Zr\text{-}Zr} \quad (3)$$

$E_{C\text{-}C}$呈现上升趋势且随着磨削距离的增加上升速度减小，同样$E_{Zr\text{-}Zr}$也呈现上升趋势，如图9所示. 相反，$E_{C\text{-}Zr}$呈现下降趋势，这表明随着磨削进行Zr原子不断地黏附在压头上，内部储存的势能通过热能的形式释放出来. 各分量的相互作用使得E_p呈先上升后下

降的趋势. 虽然不同粗糙度ZrO_2涂层各种能量的变化趋势大致相同, 但分析磨削前总势能E_{pl}与磨削后总势能E_{ph}以及总势能变化量ΔE_p, 可知随着涂层粗糙度的增加, 磨削前系统的总势能逐渐增大, 总势能的变化量逐渐减小. 本文中选用NVT系综, 系统的动能保持不变, 总势能的变化量反应了磨削时犁沟效应与黏附效应的作用强度. 这表明相同载荷下, 粗糙度增大, 磨削时犁沟效应与黏附效应都减弱, 这也导致磨损深度减小, 基体亚表面损伤程度减弱, 磨削前后总势能能量值及变化量列于表3中.

图10所示为各部分势能变化量, 由图10可知, $\Delta E_{C\text{-}Zr}$呈现下降趋势, 这表明, 随着ZrO_2涂层粗糙度的增加, 压痕深度降低, 黏附作用减弱, 磨损原子减少. $\Delta E_{Zr\text{-}Zr}$呈现下降趋势, 这表明, 随着ZrO_2涂层粗糙度的增加, Zr基体之间的作用力减少, 基体内部的塑性变形减少, $\Delta E_{C\text{-}C}$无明显变化规律.

3　结论

本文中对5种不同粗糙度的ZrO_2涂层模型进行了分子动力学摩擦磨损模拟, 研究其摩擦磨损机理, 结论如下:

a. 摩擦力和平均摩擦系数随ZrO_2涂层粗糙度的增加而呈现下降趋势, 由于压头法向与ZrO_2涂层的实际接触面积增加, 导致涂层对压头反作用力增大, 压

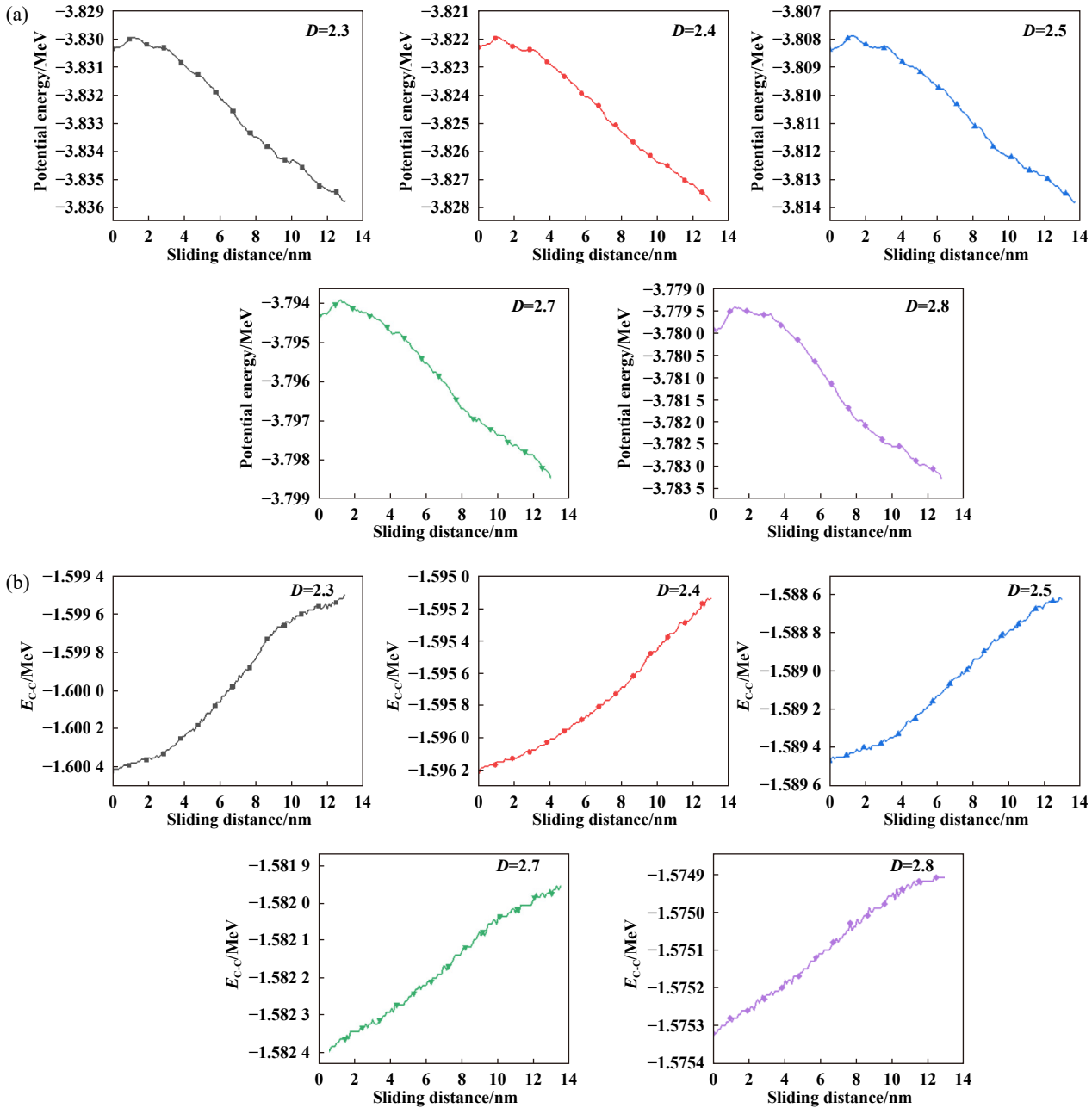

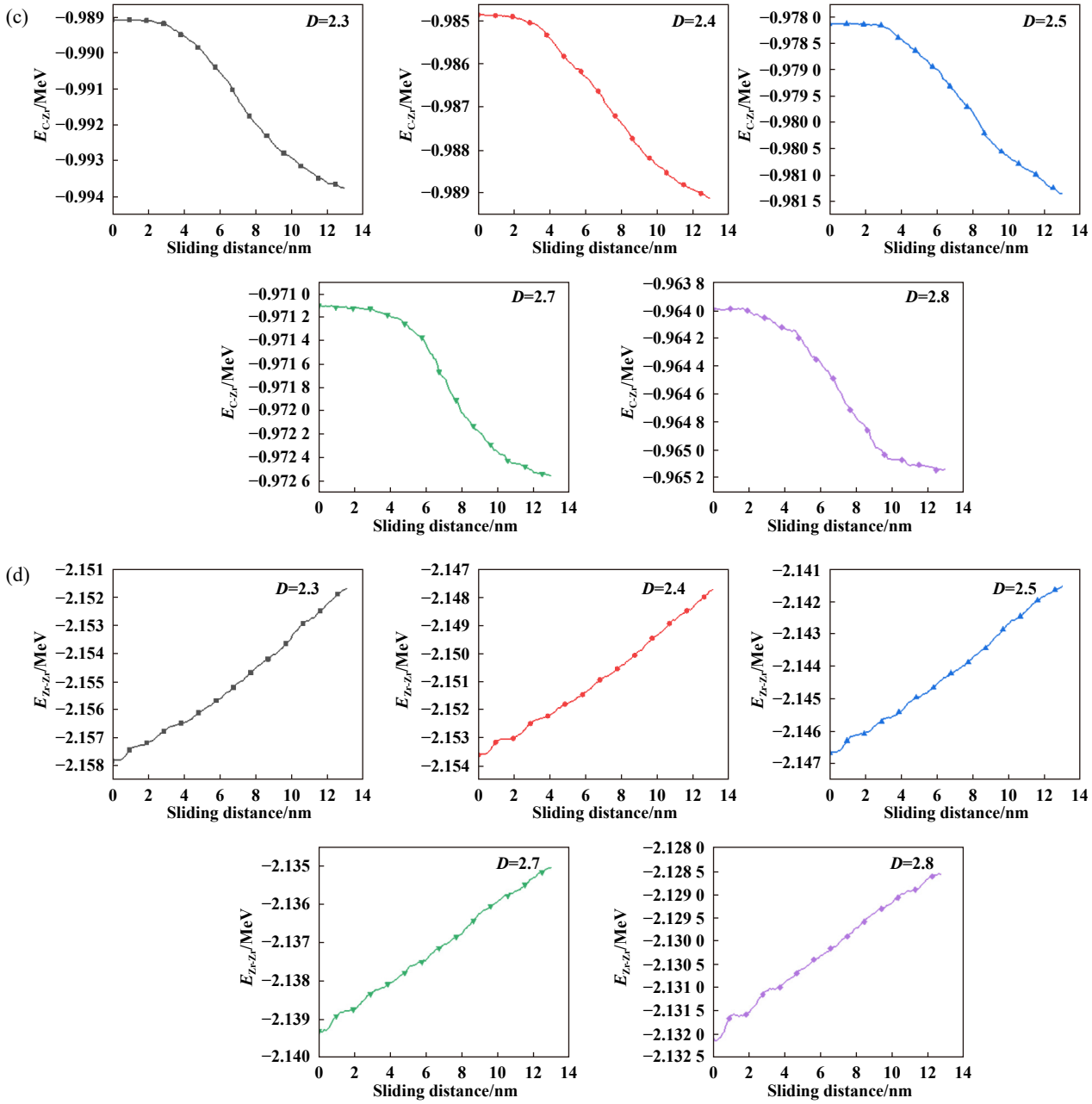

Fig. 9 Trends of potential energy changes in ZrO_2 coatings with different roughness levels: (a) total potential energy; (b) interatomic potential energy of C; (c) potential energy between C and Zr atoms; (d) potential energy between Zr and Zr atoms

图 9 不同粗糙度ZrO_2涂层势能变化趋势: (a)总势能; (b) C原子间势能; (c) C与Zr原子间势能; (d) Zr与Zr原子间势能

表 3 磨削前后总势能及变化量

Table 3 Total potential energy and changes before and after grinding

Value of D	E_{pl}/MeV	E_{ph}/MeV	ΔE_p/MeV
2.3	−3.830 35	−3.835 74	0.005 39
2.4	−3.822 18	−3.827 63	0.005 45
2.5	−3.808 17	−3.813 22	0.005 05
2.7	−3.794 34	−3.798 45	0.004 11
2.8	−3.779 93	−3.783 25	0.003 32

头磨削方向与ZrO_2涂层的实际接触面积减小，导致其相互作用力减小. 基体磨损原子量减小，磨损深度降低，磨损过程中黏附效应与犁耕效应都减弱. 表明粗糙度的增加能显著提高多晶锆表面耐磨性，减少基体亚表面的损伤.

b. 随着ZrO_2涂层粗糙度的增加，基体表面应力集中的区域更少，传递的深度更浅. 下压区域基体内部都产生堆垛层错，但基体内部晶体缺陷逐渐减少，亚表面损伤程度减弱. 总势能呈先上升后下降趋势，$E_{C\text{-}C}$

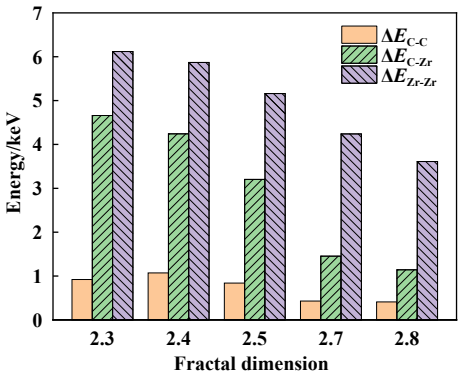

Fig. 10　Potential energy variation

图 10　势能变化量

呈现上升趋势，$E_{C\text{-}Zr}$呈现下降趋势. $\Delta E_{C\text{-}Zr}$呈现下降趋势，$\Delta E_{Zr\text{-}Zr}$呈现下降趋势，$\Delta E_{C\text{-}C}$无明显变化规律.

c. 研究表明，在设计氧化锆涂层时，在同一涂层厚度的条件下，粗糙度越高的氧化锆涂层越能增强多晶锆基体的耐磨性，降低磨削过程中基体材料的损伤程度.

参 考 文 献

[1] Bertolino G, Ruda M, Farkas D. Fracture resistance of textured polycrystalline Zr: a simulation study[J]. Computational Materials Science, 2019, 162: 304–313. doi: 10.1016/j.commatsci.2019.02.033.

[2] Tikhonchev M, Svetukhin V. Atomistic simulation of diffusion of the self-interstitial atom in HCP Zr[J]. Modelling and Simulation in Materials Science and Engineering, 2019, 27(3): 035005. doi: 10.1088/1361-651x/ab0721.

[3] Cai Zhenbing, Li Zhengyang, Yin Meigui, et al. A review of fretting study on nuclear power equipment[J]. Tribology International, 2020, 144: 106095. doi: 10.1016/j.triboint.2019.106095.

[4] Kim H G, Kim I H, Jung Y I, et al. Adhesion property and high-temperature oxidation behavior of Cr-coated Zircaloy-4 cladding tube prepared by 3D laser coating[J]. Journal of Nuclear Materials, 2015, 465: 531–539. doi: 10.1016/j.jnucmat.2015.06.030.

[5] Maier B R, Garcia-Diaz B L, Hauch B, et al. Cold spray deposition of Ti_2AlC coatings for improved nuclear fuel cladding[J]. Journal of Nuclear Materials, 2015, 466: 712–717. doi: 10.1016/j.jnucmat.2015.06.028.

[6] Alat E, Motta A T, Comstock R J, et al. Ceramic coating for corrosion (c3) resistance of nuclear fuel cladding[J]. Surface and Coatings Technology, 2015, 281: 133–143. doi: 10.1016/j.surfcoat.2015.08.062.

[7] Zhong W C, Mouche P A, Han X C, et al. Performance of iron–chromium–aluminum alloy surface coatings on Zircaloy 2 under high-temperature steam and normal BWR operating conditions[J]. Journal of Nuclear Materials, 2016, 470: 327–338. doi: 10.1016/j.jnucmat.2015.11.037.

[8] Van Nieuwenhove R, Andersson V, Balak J, et al. In-pile testing of CrN, TiAlN, and AlCrN coatings on zircaloy cladding in the halden reactor[C]//18th International Symposium on Zirconium in the Nuclear Industry, West Conshohocken, United States, 2018, 1597: 965–982. doi:10.1520/stp159720160011.

[9] Shah H, Romero J, Xu P, et al. Development of surface coatings for enhanced accident tolerant fuel (ATF)[C]//2017 Water Reactor Fuel Performance Meeting, Jeju Island, 2017.

[10] Li Wentao, Wang Zhenyu, Shuai Jintao, et al. A high oxidation resistance TizAlC coating on Zi substrates for loss-of coolant accident conditions[J]. Ceramics International, 2019, 45: 13912–13922. doi: 10.1016/j.ceramint.2019.04.089.

[11] Li Yunpeng, Song Jing, Zhang Zhiyu, et al. Research progress on mechanical properties of stabilized zirconia ceramics[J]. Materials Reports, 2022, 36(S2): 74–82 (in Chinese) [李云鹏, 宋静, 张智钰, 等. 稳定氧化锆陶瓷力学性能研究进展[J]. 材料导报, 2022, 36(S2): 74–82].

[12] Yang Hongyan, Chen Huan, Zhang Ruiqian, et al. Research progress of the surface coating for zirconium alloy cladding of accident tolerant fuel in nuclear power plant[J]. Surface Technology, 2022, 51(7): 87–97 (in Chinese) [杨红艳, 陈寰, 张瑞谦, 等. 核电耐事故锆包壳表面涂层研究进展[J]. 表面技术, 2022, 51(7): 87–97]. doi: 10.16490/j.cnki.issn.1001-3660.2022.07.008.

[13] Yan Yanqin, Qiu Changjun, Huang He. Research status of corrosion resistant coating on zirconium alloy surface[J]. Mechanical Engineer, 2018, (2): 6–8 (in Chinese) [严艳芹, 邱长军, 黄鹤. 锆合金表面耐腐蚀涂层研究现状[J]. 机械工程师, 2018, (2): 6–8]. doi: 10.3969/j.issn.1002-2333.2018.02.003.

[14] Li Zhengyang, Cai Zhenbing, Ding Yuan, et al. Characterization of graphene oxide/ZrO_2 composite coatings deposited on zirconium alloy by micro-arc oxidation[J]. Applied Surface Science, 2020, 506: 144928. doi: 10.1016/j.apsusc.2019.144928.

[15] Li Zhengyang, Cai Zhenbing, Cui Xuejun, et al. Influence of nanoparticle additions on structure and fretting corrosion behavior of micro-arc oxidation coatings on zirconium alloy[J]. Surface and Coatings Technology, 2021, 410: 126949. doi: 10.1016/j.surfcoat.2021.126949.

[16] Wang Quan, Zhuang Suguo, Liu Xiubo, et al. Molecular dynamics simulation of sliding tribological behavior of Cu-Ni alloy[J]. Tribology, 2023, 43(9): 1046–1054 (in Chinese) [王权, 庄宿国, 刘秀波, 等. 铜镍合金滑动摩擦学行为的分子动力学模拟[J]. 摩擦学学报, 2023, 43(9): 1046–1054]. doi: 10.16078/j.tribology.2022227.

[17] Wang Bing, Luo Lingzhi, Gu Bin. Molecular dynamics simulations on effect of surface texture on nano-scratch of single crystal CoCrFeMnNi high-entropy alloy[J]. Tribology, 2023, 43(7): 791–799 (in Chinese) [王冰, 罗灵芝, 古斌. 表面形貌对单晶CoCrFeMnNi高熵合金刮擦行为影响的分子动力学模拟[J]. 摩擦学学报, 2023, 43(7): 791–799]. doi: 10.16078/j.tribology.2022026.

[18] Hirel P. Atomsk: a tool for manipulating and converting atomic data

files[J]. Computer Physics Communications, 2015, 197: 212–219. doi: 10.1016/j.cpc.2015.07.012.

[19] Majumdar A, Bhushan B. Fractal model of elastic-plastic contact between rough surfaces[J]. Transactions of the ASME Journal of Tribology, 1991, 113: 1–11. doi: 10.1115/1.2920588.

[20] Ausloos M, Berman D H. A multivariate weierstrass-mandelbrot function[J]. Proceedings of the Royal Society of London Series A, 1985, 400(1819): 331–350. doi: 10.1098/rspa.1985.0083.

[21] Plimpton S. Fast parallel algorithms for short-range molecular dynamics[J]. Journal of Computational Physics, 1995, 117(1): 1–19. doi: 10.1006/jcph.1995.1039.

[22] Tersoff J. Modeling solid-state chemistry: interatomic potentials for multicomponent systems[J]. Physical Review B, 1989, 39(8): 5566–5568. doi: 10.1103/physrevb.39.5566.

[23] Mendelev M I, Ackland G J. Development of an interatomic potential for the simulation of phase transformations in zirconium[J]. Philosophical Magazine Letters, 2007, 87(5): 349–359. doi: 10.1080/09500830701191393.

[24] Zhao Yan, Zhang Yan, Liu Riping. MD simulation of chip formation in nanometric cutting of metallic glass[J]. Advanced Materials Research, 2012, 476–478: 434–437. doi:10.4028/www.scientific.net/amr.476-478.434.

[25] Lewis G V, Catlow C R A. Potential models for ionic oxides[J]. Journal of Physics C Solid State Physics, 1985, 18(6): 1149–1161. doi: 10.1088/0022-3719/18/6/010.

[26] Smith D K, Newkirk W. The crystal structure of baddeleyite (monoclinic ZrO_2) and its relation to the polymorphism of ZrO_2[J]. Acta Crystallographica, 1965, 18(6): 983–991. doi: 10.1107/s0365110x65002402.

[27] Hu X L, Martini A. Atomistic simulation of the effect of roughness on nanoscale wear[J]. Computational Materials Science, 2015, 102: 208–212. doi: 10.1016/j.commatsci.2015.02.036.

[28] Stukowski A, Bulatov V V, Arsenlis A. Automated identification and indexing of dislocations in crystal interfaces[J]. Modelling and Simulation in Materials Science and Engineering, 2012, 20(8): 085007. doi: 10.1088/0965-0393/20/8/085007.

[29] Tsuzuki H, Branicio P S, Rino J P. Structural characterization of deformed crystals by analysis of common atomic neighborhood[J]. Computer Physics Communications, 2007, 177(6): 518–523. doi: 10.1016/j.cpc.2007.05.018.

[30] Shimizu F, Ogata S, Li J. Theory of shear banding in metallic glasses and molecular dynamics calculations[J]. Materials Transactions, 2007, 48(11): 2923–2927. doi: 10.2320/matertrans.mj200769.

[31] Li Jia, Fang Qihong, Liu Youwen, et al. Scratching of copper with rough surfaces conducted by diamond tip simulated using molecular dynamics[J]. The International Journal of Advanced Manufacturing Technology, 2015, 77(5): 1057–1070. doi: 10.1007/s00170-014-6536-6.

[32] Si Lina, Wang Xiaoli, Xie Guoxin, et al. Nano-adhesion and friction of multi-asperity contact: a molecular dynamics simulation study[J]. Surface and Interface Analysis, 2015, 47(9): 919–925. doi: 10.1002/sia.5797.

[33] Zhu Kehao, Zhang Xiaoyu, Yuan Xinlu, et al. Molecular dynamics simulation of grain size effect on friction and wear of nanocrystalline zirconium[J]. Proceedings of the Institution of Mechanical Engineers, Part J: Journal of Engineering Tribology, 2021, 235(6): 1211–1221. doi: 10.1177/1350650120945079.